

# Hollow Cathode and Thruster Discharge Chamber Plasma Measurements

IEPC-2005-269

*Presented at the 29<sup>th</sup> International Electric Propulsion Conference, Princeton University,  
October 31 – November 4, 2005*

Kristina K. Jameson<sup>\*</sup>, Dan M. Goebel<sup>†</sup>, and Ron M. Watkins<sup>‡</sup>  
*Jet Propulsion Laboratory, California Institute of Technology, Pasadena, CA 91109*

**Abstract:** Due to the successful performance of the NSTAR ion thruster in Deep Space 1 mission, coupled with the recently completed 30,352 hour extended life test (ELT) of the NSTAR flight spare thruster, ion thrusters have become a viable option for future NASA missions. Proposed nuclear and solar electric propulsion missions require the life of thrusters to exceed well beyond 30,000 hours, and the life of the cathode assembly and discharge are of specific concern. In an effort to understand cathode discharge plasmas, two separate cathode geometries have been investigated: a 1/4" NSTAR cathode and a 1.5 cm NEXIS cathode. Several probe diagnostics have been used internal and external to hollow cathodes to measure the local plasma parameters. Axially scanning miniature high speed pneumatic Langmuir probes have been used to investigate the plasma parameters inside the cathode insert, in the cathode orifice and in the keeper region. For both cathodes, plasma potentials are found vary with discharge parameter and to increase gradually up to cathode orifice where a potential discontinuity exists in the orifice regions. The potential then continues to increase for several centimeters downstream of the keeper to a maximum near the anode potential. Radially-scanning emissive and Langmuir probes have also been used to obtain plasma parameters in the localized region in front of the keeper, showing that the potential is depressed on axis directly in front of the keeper and increases radially and axially as it moves through the plasma ball. In this paper, detailed measurements of the plasma parameters internal and external to the cathode will be presented for the NSTAR cathode up to 13.1A of discharge current and for the NEXIS cathode up to 30A of discharge current.

## Nomenclature

$A$	=	probe area
$e$	=	electron charge
$I$	=	probe current
$k$	=	Boltzman's constant
$M$	=	ion mass
$m$	=	electron mass
$n$	=	plasma density
$T_e$	=	electron temperature
$\square$	=	Plasma ion current coefficient

---

<sup>\*</sup> APT Staff, Advanced Propulsion Technology Group, Kristina.K.Jameson-119791@jpl.nasa.gov.

<sup>†</sup> Principal Scientist, Advanced Propulsion Technology Group, Dan.M.Goebel@jpl.nasa.gov.

<sup>‡</sup> Member of the Engineering Staff, Advanced Propulsion Technology Group, Ron.M.Watkins@jpl.nasa.gov.

## I. Introduction

Due to the successful 30,000 hour Extended Life Test (ELT)<sup>1</sup> of the NSTAR ion thruster at Jet Propulsion Laboratory and Deep Space 1 (DS1) successfully completing its mission with the NSTAR thruster as an integral part of the only on-board propulsion system, electric propulsion has now become a viable option for future NASA missions. During the post test analysis of the flight spare NSTAR thruster, it became apparent that erosion of the hollow cathode assembly has become a major life limiting mechanism for electric propulsion systems. However, the hollow cathodes appear to be the least well understood of all the components in the thruster. After nearly 40 years of investigation and decades of use in thrusters, there are no definitive models of the plasma density, temperature and potential distributions capable of describing different thermionic hollow cathode configurations and discharge conditions, and only limited empirical data of the geometry dependence on the life and performance. In order to understand hollow cathode discharges, we have undertaken a probe study of the cathode, keeper and cathode-plume regions. Fast axial and radial scanning probes are used to produce profiles of the plasma density, potential and temperature for different discharge currents and gas flow rates. This data aids in a basic understanding of the hollow cathode physics and will ultimately assist in determining cathode life.

Probing of thermionic hollow cathodes has been performed since they were invented by Lidsky<sup>1</sup> in the 1962. Familiar thermionic hollow cathode geometries were described by Rawlings<sup>2</sup> for mercury thrusters, Moore<sup>3</sup> for cesium thrusters, and Sovey<sup>4</sup> for noble-gas magnetic-cusp thrusters. The definitive probe study of a mercury hollow cathode was performed by Siegfried and Wilbur<sup>5</sup> in 1978. In this study, moveable probes were placed in different positions in the insert region and in the keeper/plasma plume region of a mercury cathode operated without an applied axial magnetic field. Moving the probes to new positions in steps produced profiles of density, potential, and temperature. Since the probes were of significant size to avoid melting and were moved into position manually and were stationary during data acquisition, the region near the cathode orifice was unreachable and the discharge was limited to currents below about 10 A. However, densities in excess of  $1 \times 10^{14} \text{ cm}^{-3}$  were measured in the hollow cathode and axial profiles of these plasma parameters away from the cathode orifice for spot mode and plume modes operation were obtained. Hayakawa<sup>6</sup> published in 1989 probe data downstream from a hollow cathode in a 14 cm ring-cusp thruster, and found evidence of primary electrons in the distribution function. These experiments provided data within 1.6 cm of the cathode, but did not approach the keeper or cathode-orifice regions.

Recently, cathode and thruster discharge parameters have been investigated inside NSTAR flight-like thrusters using single and double Langmuir probes by Herman<sup>7,8</sup> and Sengupta.<sup>9</sup> Herman investigated the keeper region radially as close as 1.5 mm in front of the keeper out to 4 cm downstream using a reciprocating probe with dwell times in the plasma less than one second. Herman has also used emissive probes in the cathode plume region to find plasma potentials from 1.5 mm to 2 cm downstream of the keeper.<sup>10</sup> Sengupta investigated plasma parameters radially over a larger area inside the thruster, 1 cm in front of the keeper to 10 cm downstream, with a scanning probe that had dwell times also less than one second.<sup>9</sup> None of these investigations were capable of obtaining the plasma parameters inside the hollow cathode and in the orifice region of the keeper.

To diagnose the local plasma parameters inside the cathode, the cathode plume, and discharge chamber, a mock up of the NSTAR thruster discharge chamber was assembled in the JPL cathode test facility<sup>11,12</sup>. The experimental setup consists of cathode station, where either a 1/4" NSTAR cathode or a 1.5-cm NEXIS cathode is mounted, a water-cooled anode that simulates the 30-cm thruster body, and various diagnostics inserted into the plasma. Two small, minimally-perturbing Langmuir probes are driven axially in the system by high speed pneumatic plungers with speeds as high as 2 m/s. This fast scanning speed is required because these regions typically have high plasma densities, which can cause the small probes to over heat and melt. The cathode probe, constructed with a 0.5 mm dia. ceramic tube at the tip, is capable of being inserted from the upstream edge of the insert all the way through the cathode orifice entrance and into the keeper region. The peak plasma density inside the NSTAR hollow cathode is in the low  $10^{15} \text{ cm}^{-3}$  range while the NEXIS cathode is in the low  $10^{14} \text{ cm}^{-3}$  range. In the anode region the density for both cathodes are in the  $10^{11}$ - $10^{13} \text{ cm}^{-3}$  range, depending on the distance from the cathode exit. Axial potential profiles internal to the NSTAR cathode are found to be relatively constant over the 3-to-5 mm plasma contact length, with a 6 V plasma potential for TH15 and a 9 V plasma potential for TH8. The potential decreases gradually upstream of this region. The NEXIS cathode potential profile is also relatively constant at 12 V for the nominal 25 A case and as much as 20 V for the 10 A case. The similarly constructed anode probe has a throw of up to 15 cm and can insert a Langmuir probe from the exit of the anode cylinder into the orifice of the keeper. The anode potentials vary from a low potential on the order of 12 to 18 V in the cathode and keeper orifice region, which increases to a higher potential on the order of the plasma potential 2-to-5 cm downstream for both cathodes. The different NSTAR and NEXIS operation levels impact both the cathode and anode potential profiles; however the

electron temperature is not very sensitive to the operating condition. The temperature is less than 2 eV internal to the NSTAR cathode and 2-3 eV internal to the NEXIS cathode. The electron temperature typically is found to increase from 2-3 eV in the keeper orifice to 4-5 eV downstream for both cathodes. In this paper, detailed measurements of the plasma parameters will be presented inside the cathode and in the keeper and discharge chamber regions for the NSTAR cathode at TH8 and TH15 throttle levels and the NEXIS cathode at 10 A and 25 A operation conditions.

## II. Experimental Hardware

A schematic illustration of the hollow cathode, anode, cathode and anode probe assemblies, and the radial probe is shown in Figure 1. Two different hollow cathodes are used in these experiments, a conventional NSTAR cathode and a NEXIS cathode. The conventional NSTAR cathode<sup>13</sup> is constructed with a 6.35-mm diameter molybdenum-rhenium tube with a thoriated tungsten plate welded to the downstream end. This plate has a small orifice, of order 1 mm diameter, located on the centerline of the cathode. The NEXIS cathode has a configuration of a 1.5 cm diameter molybdenum tube with a tungsten orifice plate e-beam welded on the end, with an orifice size on the order 2-3 mm.<sup>11</sup> A porous tungsten insert impregnated with a low-work-function barium-calcium-aluminate mixture is placed inside both the NSTAR and NEXIS cathodes.<sup>11,14</sup> Electrons are emitted from this insert by field-enhanced thermionic emission ionize the neutral xenon gas inside the cathode. Electrons from this plasma are extracted at the downstream boundary and travel through the cathode orifice before entering the main discharge. The cathodes are heated by a standard co-axial sheathed heater, which is turned off during discharge operation. A graphite keeper electrode fully encloses both of the cathodes, and the keeper orifice is about 4.6 times the diameter of the cathode orifice for NSTAR and about 1.7 times the cathode orifice for NEXIS. The cathode and scanning probe system are mounted on an 8" Conflat flange installed in one port of 0.75-m diameter, 2-m long vacuum chamber. The chamber is pumped by two 10" CTI cryopumps with a combined xenon pumping speed of 1275 l/sec for xenon. The base pressure of the chamber is in the  $1 \times 10^{-8}$  Torr range, and during normal operation at less than 10 sccm of xenon flow the chamber pressure remains in the  $10^{-5}$  Torr range.

The cathode scanning probe assembly is shown in Fig. 2, and a photograph of this assembly is shown in Fig. 3a. The bellows isolated pneumatic plunger for the cathode probe (not shown) is mounted to the mini-conflat flange exterior to the chamber. The pneumatic drive shaft is coupled inside the vacuum chamber to a bellows mounted between an SMA feedthrough flange connected to the probe and a six-way mini-conflat cross. Actuation of the plunger moves the SMA flange on a linear slide, compresses the bellows and inserts the single Langmuir probe into the hollow cathode. The xenon gas is controlled and measured by a digital MKS mass flow controller and injected

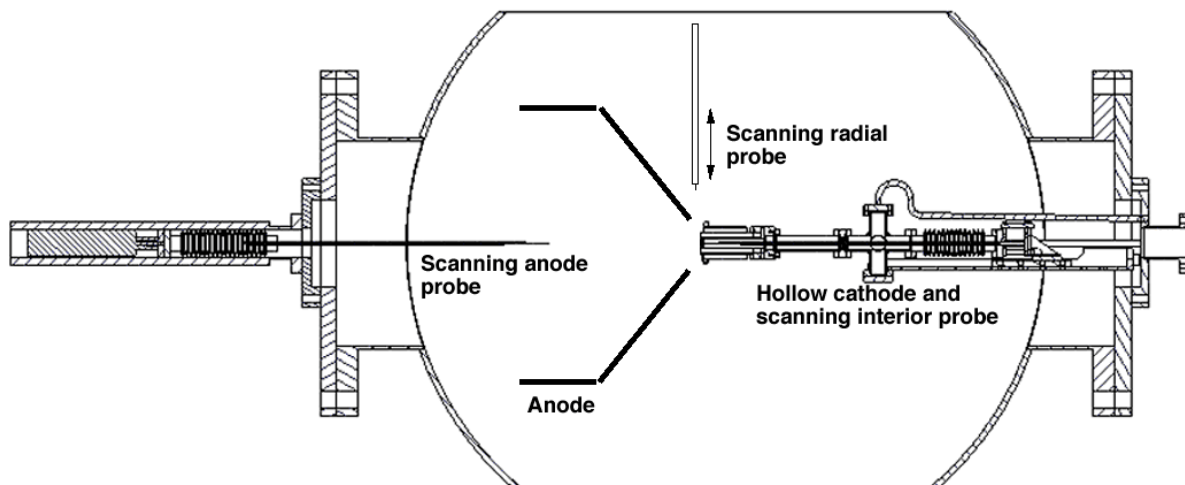


**Figure 1. Schematic drawing of the cathode and anode placement along with the pneumatic scanning probes relative to the vacuum chamber.**

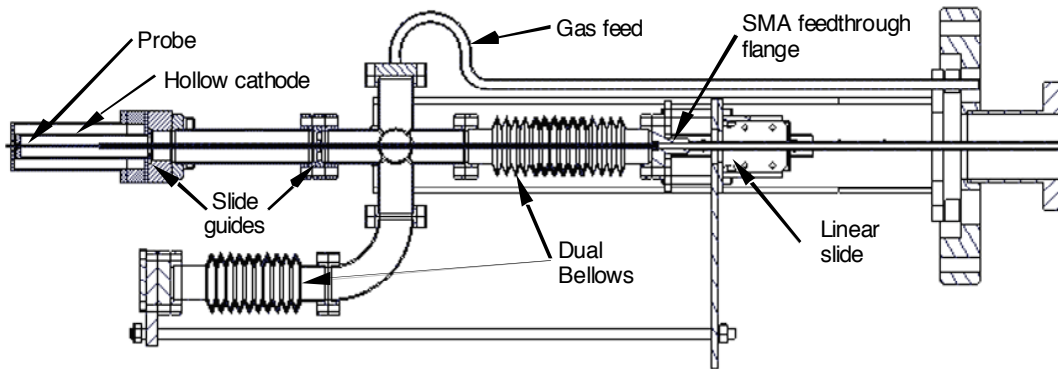


**Figure 2. Schematic drawing of the pneumatic scanning probe and dual bellows arrangement used to measure the plasma parameters and pressure in the hollow cathode.**

into the hollow cathode through one port on the six-way cross. Since the plunger action will change the pressure inside the hollow cathode by decreasing the volume of the enclosed system, a second bellows on another linear slide arrangement is mounted on one of the six-way-cross ports. This second bellows is coupled to the first such that compression of the primary bellows causes a proportional expansion of the second bellows to maintain a constant volume in the system so that the pressure in the hollow cathode region is not changed during the fast probe insertion. A third port on the six-way cross is connected to a precision Baratron capacitive manometer to measure the pressure in the hollow cathode during operation.

A photograph of the cathode probe tip extending through the NEXIS cathode orifice is shown in Figure 3b. The probe tip is 0.5 mm diameter alumina tubing with a 0.127 mm diameter tungsten wire electrode that protrudes from the small-bore ceramic tubing a distance of 0.25 mm. Even though the wire electrode is kept at a minimal length for electron collection, the probe has collected up to 5 A of current in the high density region near the orifice of the NSTAR cathode. The cathode probe is aligned axially in the system by two slide-guides internal to the cathode system. The cathode probe has a linear throw of 4 cm and can traverse the cathode at over one meter per second with a resolution of 0.25 mm. The probe tip occupies about 25% of the NSTAR cathode orifice cross sectional area, and significantly perturbs the plasma discharge if the probe is pushed too far past the upstream orifice entrance. For this reason, data is only taken prior to the probe entering the cathode orifice. Since the NEXIS cathode has a significantly larger cathode orifice, the probe tip occupies less than 3.5% of the orifice area and does not significantly perturb the plasma discharge, therefore information can be obtained inside the cathode orifice and in

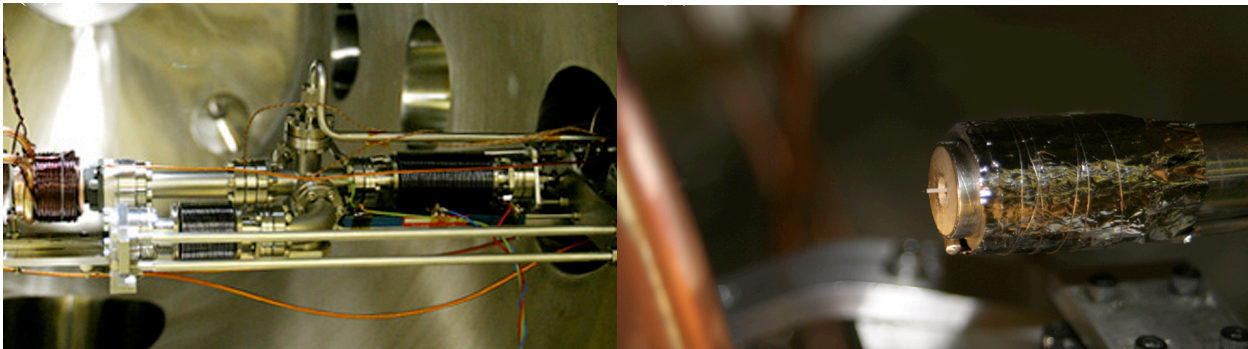


**Figure 3. Scanning probe assemblies (a) cathode probe drive system mounted in the vacuum chamber, and (b) the cathode probe tip shown sticking out of the NEXIS orifice.**

the region between the cathode and the keeper. Also shown in Fig. 3a is a solenoid coil wound on a water cooled cylinder directly around the cathode to provide an axial magnetic field of adjustable amplitude at the cathode exit that simulates the cathode field in ring-cusp thrusters. A full description of the cathode probe assembly is presented in reference 11.

The anode scanning-probe assembly is shown in Figure 4a, where the pneumatic plunger and vacuum bellows arrangement mounted on the outside of the vacuum system are seen. The diameter of the ceramic tubing interior to

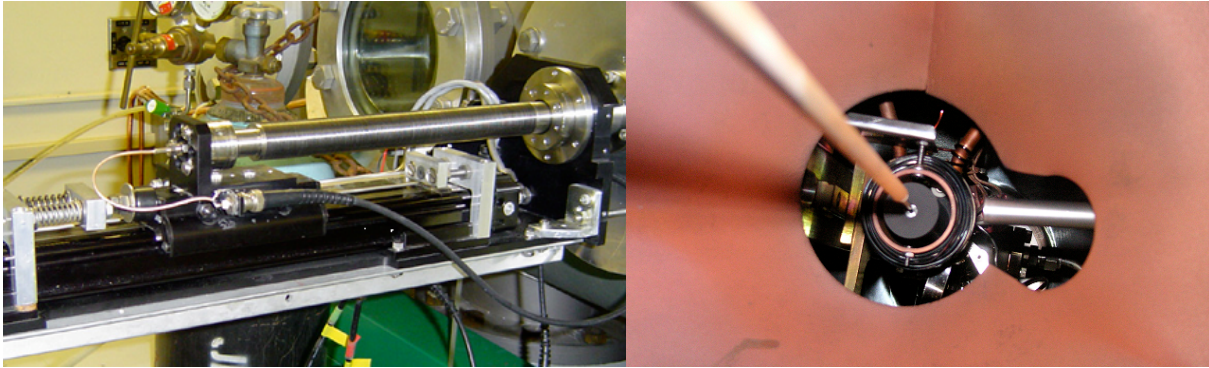


**Figure 4. Scanning probe assemblies (a) anode probe drive system mounted external to the vacuum chamber, and (b) the anode probe shown entering into the NSTAR keeper region.**

the vacuum system is stepped down from 3 mm to 0.5 mm diameter in the last 3-cm section that is inserted deepest into the plasma in order to minimize perturbation to the plasma in the anode region. The exposed electrode is again a 0.127 mm tungsten wire, but has a length of typically 1 mm to collect sufficient current away from the keeper region to accurately determine the plasma parameters. The anode probe has nearly three times the throw of the cathode probe and 5 times the unsupported length so as to not perturb the anode-plasma, and usually moves at one meter a second with a position resolution of 0.5 mm. Very careful iterative alignment techniques are used to ensure that the anode probe is aligned with the cathode orifice and within 0.5 mm of the centerline. The anode probe can be fully inserted into the keeper orifice, although whip of the long ceramic sometimes causes the tip to touch the keeper or cathode during retraction. The anode probe inserting through the entrance of the anode and into the keeper region of a NSTAR cathode can be seen in Fig. 4b.

A radially scanning probe is also schematically shown in Fig. 1. This probe can be configured either as an emissive probe or as a Langmuir probe. It uses a pneumatic plunger external to the vacuum system, identical to the cathode-probe plunger, and is mounted to a Huntington X-Y manipulator outside the vacuum system to provide positioning relative to the keeper exit point. The radial probe has a linear throw of 4 cm, also at about one meter per second, and is aligned by a slide-guide internal to the vacuum system to obtain a position resolution of 0.25 mm. The probe can be positioned in front of the keeper as close as 1 mm out to 2.5 cm downstream. The emissive probe tip is a 0.127-mm diameter tungsten hairpin wire fed through two side-by-side 0.5 mm diameter alumina tubes. A floating 5 amp power supply provides the current to heat the tungsten wire electrode to emit electrons. The Langmuir probe tip is a 0.127 mm diameter tungsten wire occupying only one 0.5 mm diameter alumina tube with a probe tip length of 1 mm. The probe tip length is set to collect sufficient current in the lower density region external to the cathode, but is still relatively short as to not over heat and melt the probe tip in the high density region directly in front of the cathode orifice. When the radial probe is not in use, it is

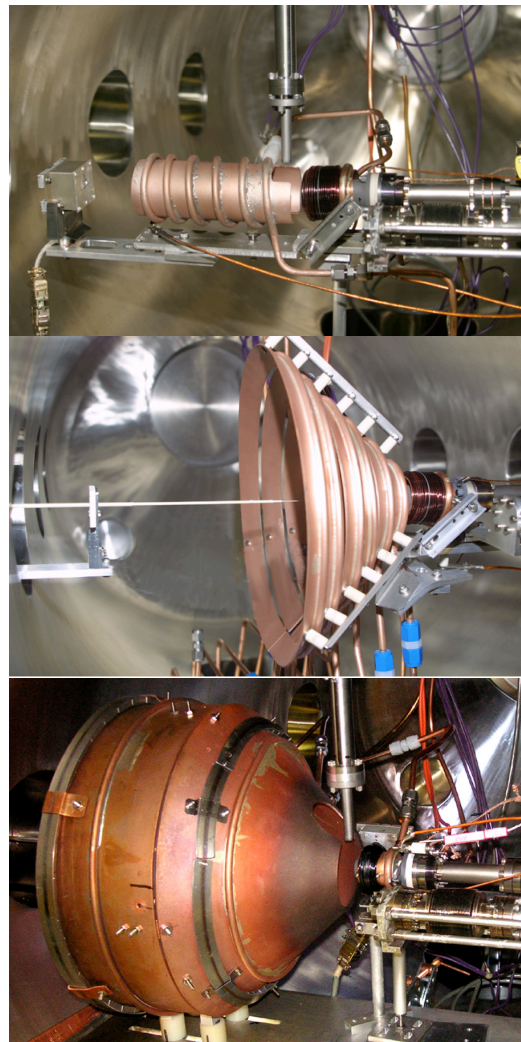


**Figure 5. Water-cooled anode geometries (a) cylindrical anode (b) segmented conical anode and (c) NSTAR-like conical-cylindrical anode.**

retracted into a 6.5 mm tube that is sufficiently out of the discharge plume to protect it from ion bombardment.

In order to take Langmuir traces, a bias voltage is applied to the probe tips, which is generated by a programmable waveform synthesizer that drives a Kepco bipolar power supply. The voltage waveform is a sawtooth ramp that scans from  $-10$  to  $+50$  V in the anode region and from  $-10$  to  $+30$  in the cathode region in a time of 1 msec. In the NSTAR cathode, the cathode probe voltage is swept once per insertion to avoid overheating the probe tip in the high-density plasma near the hollow cathode orifice. A delay generator is used to take consecutive traces allowing the cathode plasma parameters can be mapped. In the NEXIS cathode, a series of voltage ramps are utilized to map the plasma parameters in a single insertion. Electron temperatures and plasma potentials are determined in less than half of the total 1 msec trace therefore the position uncertainty for the plasma parameters is on the order of 0.5 mm over most of the scan and less than 0.25 mm near the full insertion point. The probe position, voltage and current data is collected on a PC at a sample rate of 300 kHz, resulting in 300 data points in each probe characteristic curve. The plasma potential and electron temperatures are found by classical Langmuir probe analysis. The electron temperature is found by fitting an exponential curve to the electron retardation region of the Langmuir trace. The electron temperatures have error bars about 0.5 V and the plasma potentials have error bars of  $\pm 1$  V in the cathode region and up to  $\pm 2$  V in the anode region.

The experimental arrangement accommodated three different anode geometries, with all anode geometries made out of cooper and water-cooled. The first geometry, being the simplest, was a cylindrical anode 5 cm in diameter and about 12 cm long. Experiments with the cylindrical anode demonstrated stable discharge for the NEXIS cathode at currents of 5 to 35 A were possible at corresponding cathode flow rates in the range of 3 to 8 sccm. At the nominal discharge current from the current-controlled power supply of 25 A and the nominal flow rates from the regulated gas system of 5.5 sccm, the discharge voltage was found to be only about 16 V. Since typical thrusters operate in the neighborhood of 25 V, it was decided to modify the anode geometry to the second geometry, a conical shape similar to the rear of NSTAR-type thrusters to raise the discharge voltage. Figure 5a shows a picture of the cylindrical anode while Figure 5b shows a picture of the segmented conical anode. The segmented conical anode was constructed of six isolated segments so that the current distribution could be measured as a function of the total discharge current, flow rate and magnetic field strength. This arrangement can produce discharges at 10 A at 27.3 V and at 25 A at 26.3 V. In order to accommodate the NSTAR cathode with a more representative three ring cusp magnetic field for a stable discharge, a third anode geometry was constructed, which can be seen in Figure 5c. The third geometry has a conical section with a minimum diameter of approximately 5 cm, and is joined to the 30-cm-dia. straight cylindrical section. Also there is an adjustable gap of typically about 2 cm between the anode and keeper, thus allowing for visualization of the cathode plume and to acquire radial emissive and Langmuir probe traces. There is a solenoid coil positioned around the cathode to produce an axial magnetic field, along with two rings of permanent magnets around the anode body to simulate the NSTAR magnetic field geometry following the north-south-north structure. This anode geometry is capable of reproducing the full NSTAR Throttle Table with an emphases placed on TH8 and TH15. This arrangement can produce discharges at 8.2 A at 26.3 V representing TH8 and 13.1 A at 25.6 V representing TH15.

### III. Experimental Results

The pressure inside the hollow cathode is measured by a Baratron manometer and recorded for different operating conditions. Internal cathode pressure for the NSTAR throttle levels is shown in Fig. 6. The neutral pressure inside the hollow cathode is relatively high for the NSTAR cathode, starting from about 4 Torr at TH4 and increasing to over 8 Torr for TH15. Even at TH4 the neutral pressure is sufficiently high to cause the plasma inside the cathode to be dominated by collisions. The flow rate is constant for TH4 and TH8, so the increase in pressure observed is due to the higher discharge current at TH08 which is heating

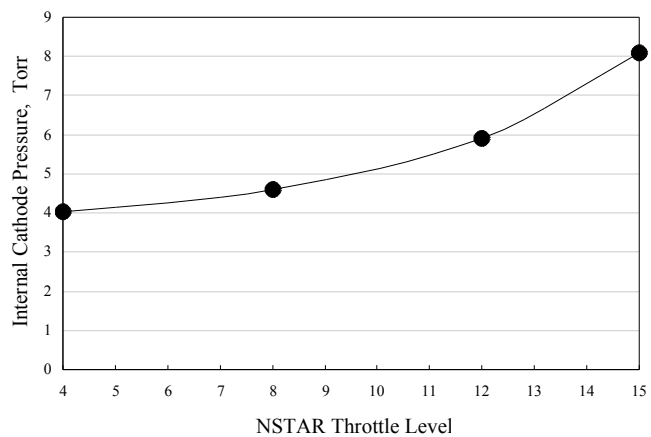
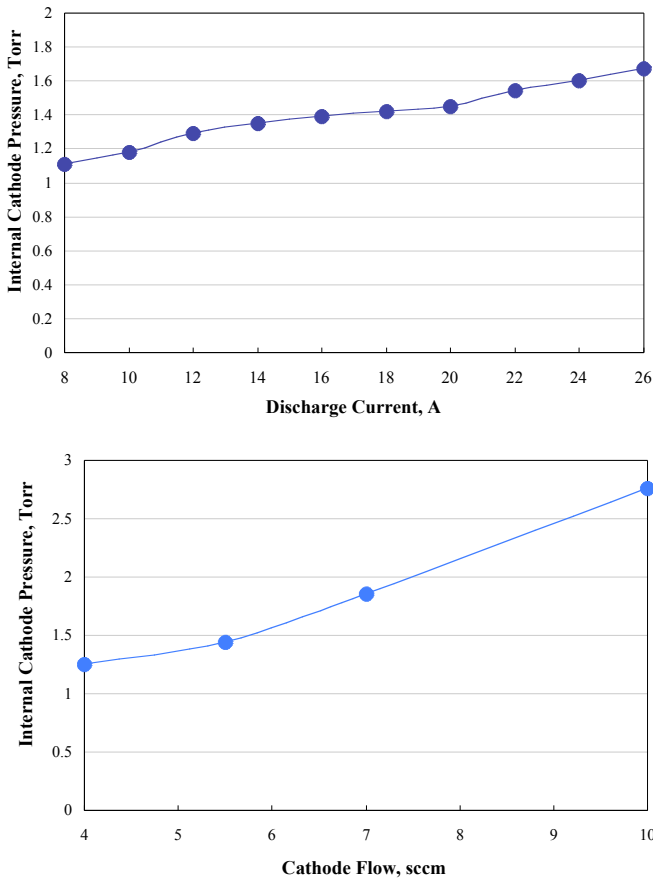


Figure 6. Pressure measured inside the 1/4" hollow cathode for various NSTAR throttle levels.



**Figure 7. Internal NEXIS cathode pressure (a) constant flow rate at 5.5 sccm (b) constant discharge current at 22 A.**

the gas. As the flow rate and discharge current are increased from TH8 through TH15, the pressure increases significantly causing the plasma inside the cathode to become even more collisional as the throttle level is increased. The internal pressure for the NEXIS hollow cathode is shown in Figure 7; where Fig. 7a shows the internal pressure for constant flow rate at 5.5 sccm, while Fig. 7b shows the internal pressure for constant discharge current at 22 A. The NEXIS cathode shows the same trend as the NSTAR cathode; when the discharge current is increased the gas is being heated and causes the internal pressure to increase almost linearly, from 1.3 Torr at 8 A to 1.7 Torr at 26 A. Keeping the discharge current constant and increasing the flow rate shows a more significant pressure increase, from 1.25 Torr at 4 sccm to 2.75 at 10 sccm. As flow rate is increased, the gas internal to the cathode becomes more collisional due to a higher amount of gas is being pushed through the same size orifice. However, the pressure inside the NEXIS cathode is always noticeably lower compared to the NSTAR cathode. While at TH4, which is at 2.47 sccm, the pressure inside the NSTAR cathode is a 4 Torr, the pressure inside of the NEXIS cathode is only at 2.75 Torr at 10 sccm. Due to the orifice size, the NEXIS cathode runs in a different collisionality regime than the NSTAR cathode that is always very collisional. At nominal operation of the NEXIS cathode which is 25 A at 5.5 sccm the pressure is only 1.5 Torr which causes the cathode to run at a lower temperature.

### A. Density Measurements

The plasma density in the cathode and keeper regions is found from taking position scans with the Langmuir probe biased to ion saturation current. In this region, the plasma density is sufficiently high that the sheath is small compared to the probe radius and the probe data can be analyzed in the “thin-sheath” regime. The plasma density in the thin sheath regime is evaluated from the current<sup>15,16</sup> given by:

$$I = \square n e \sqrt{\frac{kT_e}{M}} A \quad (1)$$

where  $\square$  is a coefficient that changes with the geometry and the collisionality of the plasma,  $n$  is the density,  $e$  is electron charge,  $kT_e$  is the electron temperature,  $M$  is the ion mass, and  $A$  is the area of the probe. If the plasma is in a collisionless regime,  $\square$  is given as 0.5 from the Bohm current<sup>15,16</sup>. If the plasma is in a collisional regime  $\square$  ranges from 0.38 to 0.8 depending on the collisionality.<sup>16</sup> Since the neutral pressure inside of the NSTAR hollow cathode is very high for the all throttle level cases as shown in Figure 6, the value for  $\square$  was chosen to be 0.8. While the neutral pressure for NEXIS cathode is significantly lower,  $\square$  was chosen as .5. The appropriateness of the probe theory used (thin or thick sheath) is checked periodically by calculating the ratio of the Debye length to the probe radius. The plasma density enters the thick sheath regime in the anode region approximately 3 cm downstream from the keeper,

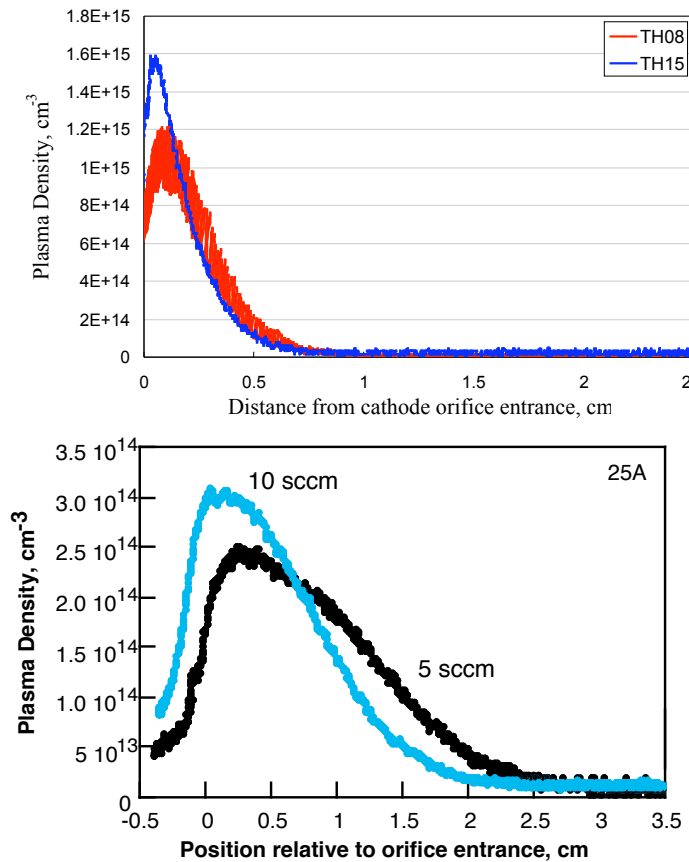


**Figure 8. Cathode density profiles plotted on a linear scale for (a) the NSTAR cathode (b) the NEXIS cathode.**

also be seen in Figure 8b, for the NEXIS cathode. The neutral pressure for the 10 sccm case is 1.7-1.9 times that of the 5.5 sccm case, which also causes the peak density to be pushed farther downstream closer to the cathode orifice. The plasma contact area with the insert thereby decreases, suggesting that cathodes operated at pressures in the few Torr range may only utilize a fraction of the insert length for significant electron emission.<sup>11</sup> Surprisingly the signal for the TH8 case is much noisier than that for the TH15 case. This was also true when the probe was used to measure the floating potential. In the anode region, neither the floating potential or the ion saturation current signal were significantly more noisy for TH8 compared to TH15. It appears that the plasma in the cathode and keeper orifice regions for TH08 is inherently less stable than for TH15, probably due to the combination of gas flow and discharge current selected for this mode. The NEXIS cathode did not show any instability in the probe signal for either operation condition, suggesting that the cathode design is sufficient for the higher flow rates nominal discharge current of 25 A for this cathode.

The plasma density profiles measured inside the cathode are not only affected by the discharge current and cathode flow rate, it is also affected by the orifice size. Different NEXIS cathode geometries were manufactured and tested. Shown in Fig. 9 are the density profiles internal to the NEXIS cathode for two different orifice sizes at 5.5 sccm and 10 sccm. Both NEXIS cathodes show the higher flow rate causes the density peak to be pushed downstream closer to the orifice, however the peak for the 2 mm orifice is about 2-3 mm downstream of the peak for the 2.8 mm case. In the smaller orifice NEXIS cathode, the orifice occupies about 20% of the diameter the cathode tube where the larger orifice occupies 30% of the cathode tube. Compared to the NSTAR cathode where the orifice occupies 15% of the cathode tube, the peak density is very close to the orifice, the large orifice NEXIS cathode occupies twice that of the NSTAR cathode allowing the peak density to be upstream of the orifice by 4-5 mm. When the orifice size is smaller relative to the cathode tube, it is more difficult for the plasma to escape through the

where the density falls almost an order of magnitude relative to the keeper exit. When the miniature probe is found to be taking data in the thick sheath regime, a larger radius electrode is used in the anode probe to ensure that more reliable thin sheath theory can be used. If the appropriate theory for analysis cannot be definitely determined and accurate results obtained, the data is discarded. Also, the electron temperature used for evaluating the density is obtained from the Langmuir probe data as described before.

The NSTAR throttle table is designed to keep the discharge voltage constant in the thruster while the flow rate and/or the discharge current is increased when moving from a low throttle level to a high throttle level.<sup>14</sup> When changing operating conditions from TH8 to TH15, which increases in both discharge current and flow rate, the density profile is shifted downstream toward the orifice and is steeper, shown in Figure 8a. Peak plasma densities in this cathode routinely reach the low  $10^{15}$   $\text{cm}^{-3}$  range for TH 15, which is about 1.5 times larger than the TH8 peak density. The neutral pressure inside the cathode for TH15 is 1.6-1.7 that of TH8 which has an affect on the profiles. Higher neutral pressures in the insert region are observed to cause the cathode plasma density to decrease more rapidly upstream from the orifice. The peak plasma location is shifted downstream toward the orifice for TH15. This effect can

orifice into the main cathode plume, causing the density peak to closer to the orifice plate. Thus, the smaller the orifice relative to the cathode tube, causes the orifice plate to run at a hotter temperature.<sup>17</sup>

The plasma density profiles measured by the cathode and anode probes are shown in Figure 10a and 10b for both the NSTAR cathode and NEXIS cathode, respectively. The data for the anode region shows that the density for TH15 is 2 times larger than the density for TH8, and both density profiles fall an order of magnitude as the probe traverses downstream of the keeper. On the other hand, inside the cathode the density varies by 3 orders of magnitude as the probe moves upstream of the cathode orifice. Beyond 1 cm upstream of the cathode orifice, there is very little plasma density and do to limitations of the of the cathode probe, just bit noise is detected by the probe. We expect the density to fall in the manor shown by the two solid lines extending from the density curves in the cathode region. Future plans are to obtain density profiles in the cathode for the full insert length. The NEXIS data was taken with segmented conical anode, however data is only taken 6 cm downstream of the cathode orifice, in these 6 cm both the NSTAR-like anode and the segmented conical anode has the same geometry, so the data is comparable. The anode data for the

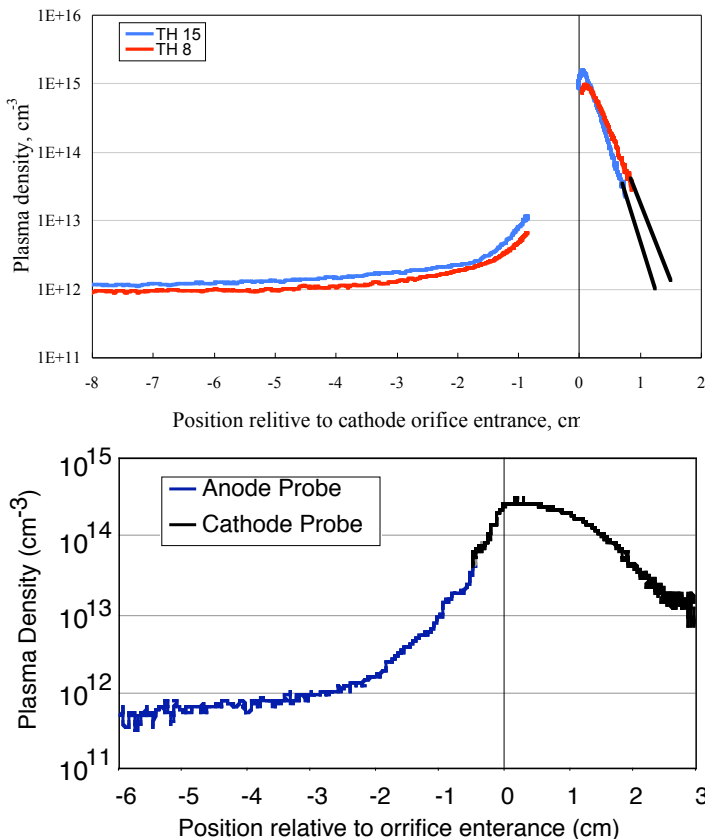


**Figure 10. Axial density cathode and anode profiles plotted on a semi-log scale (a) for the NSTAR cathode (b) for the NEXIS cathode.**

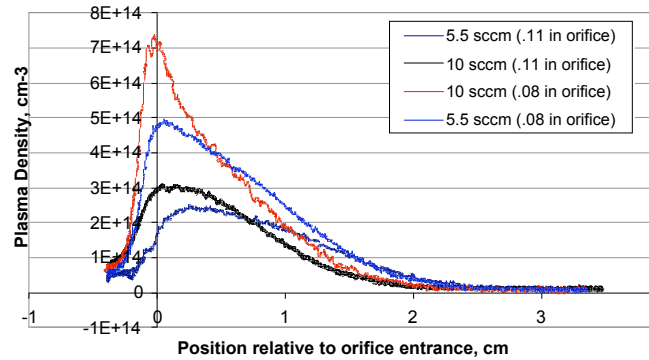


**Figure 9. Axial cathode density profiles for the NEXIS cathode for two different orifice sizes.**

The NEXIS cathode shows that the density falls almost three orders of magnitude, while the NSTAR only falls one order. The cathode density profile also differs for that of the NSTAR cathode. Where there was not sufficient plasma to measure the density upstream beyond 1 cm, the NEXIS cathode had sufficient plasma with the same probe 2.5 cm upstream. The NEXIS cathode utilizes the length of the insert where as the NSTAR cathode density is concentrated in the first centimeter upstream of the orifice. The density inside of the NEXIS cathode for 25 A at 5.5 sccm is almost order of magnitude lower than the density for TH15 in NSTAR. The cathode tube diameter and orifice affects the density internal to the cathode as described, but it also affects the anode density profile. For the NEXIS cathode, the entire density profile could be obtained, unlike the NSTAR cathode for limitations on the probe tip size as mentioned previously. Even with these limitations, the density could be obtained at the cathode orifice entrance of the NSTAR cathode, which is almost an order of magnitude higher than that of the NEXIS cathode. At one centimeter downstream of the orifice entrance, the magnitude of the plasma density is also an order of magnitude lower. The plasma in both cases occupies the same volume, therefore for the NEXIS cathode the plasma density falls

faster than the plasma density in the NSTAR case.

### B. Plasma Potential and Electron Temperature Measurements

The axial plasma potential and temperature profiles for the cathodes are shown in Figure 11, NSTAR in 11a and NEXIS 11b. In Figure 11a, the plasma potential inside the hollow cathode on axis is found to increase slightly from 4.5 V from 1 cm upstream to about 6.5 V from 0.1 cm upstream of the orifice for TH15. In the orifice the potential increases, but the perturbations to the discharge by the probe made investigating this area difficult. At TH8, the plasma potential is significantly higher than in TH15, with the potential reaching 10 V at the orifice entrance. The plasma potential in the orifice region should also increase for the TH8 case, but inserting the probe into the orifice significantly perturbed the already unstable discharge at this mode and a reliable potential measurement in the orifice could not be made. The increase in plasma potential inside the insert region at the lower TH08 discharge current clearly shows that the cathode adjusts the internal potential drop to provide adequate self-heating. At lower discharge currents, higher potential drops are needed to produce the required cathode temperature to supply the electron emission needed to support the discharge current set by the current controlled power supply. Figure 11b shows the potentials for the nominal discharge current for the NEXIS cathode. At 25 A, the potential on axis is relatively constant at about 13 V and at the orifice the potential jumps to about 16 V. As mentioned previously the probe geometry for the NEXIS cathode allowed measurements in the orifice and into the keeper, which Figure 11b shows that the potential continues to increase to nearly 20 V at the keeper orifice. The effect of higher flow rates at the same discharge current, shows that the potential drops about 3 V on axis and decreases less upstream where the insert is not used as efficiently, but the potential profile for 25 A at 10 sccm follows the same trend by increasing in potential in the keeper orifice to about 17 V. Increasing the gas flow rate at a fixed discharge current always decreases the discharge voltage and the electron temperature measured throughout the system. Figure 11b also shows that the NEXIS cathode is self-heating, in which at lower discharge currents the potential increases to 20-25 V in the insert region.

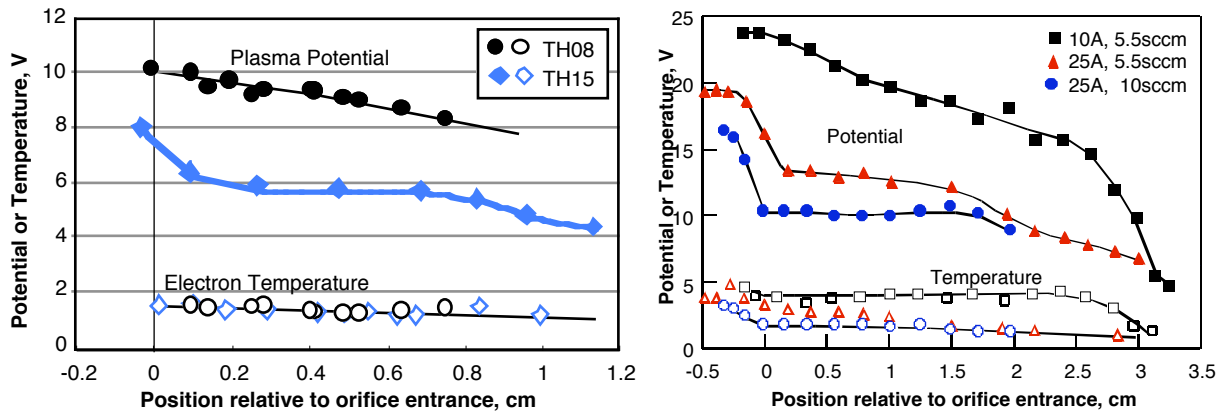


**Figure 11. Plasma potential and temperature profiles for (a) for the NSTAR cathode and (b) for the NEXIS cathode.**

The potential and temperature distributions for the anode in the keeper region for TH15 and TH8 are shown in Fig. 12 along with the corresponding cathode plasma profiles. The anode probe can be inserted into the keeper orifice but not much farther without sometimes striking the cathode orifice plate, so there is still a discontinuity in the data from the cathode probe to the anode probe. Like the cathode profiles, the anode plasma potentials are dependent on the throttle level, while the electron temperatures are very similar for both throttle levels. The potential profile for TH15 shows a clear potential discontinuity, where the potential increases from about 6.5 V at the cathode orifice entrance to 12 V just inside of the keeper orifice. The potential for TH8 also shows a potential discontinuity of approximately 4 V from the cathode orifice to the keeper orifice. The TH15 potential profile is constant for about 2mm inside keeper orifice and continues to increase downstream of the keeper. In comparison, for TH8 the potential is constant over about 5 mm through the keeper orifice and then there is another plasma discontinuity slightly downstream but with only a 2 V difference. However in TH8 the flow rate is low, the plasma density is low, and the plasma does not have enough energy to produce sufficient plasma to conduct the current to

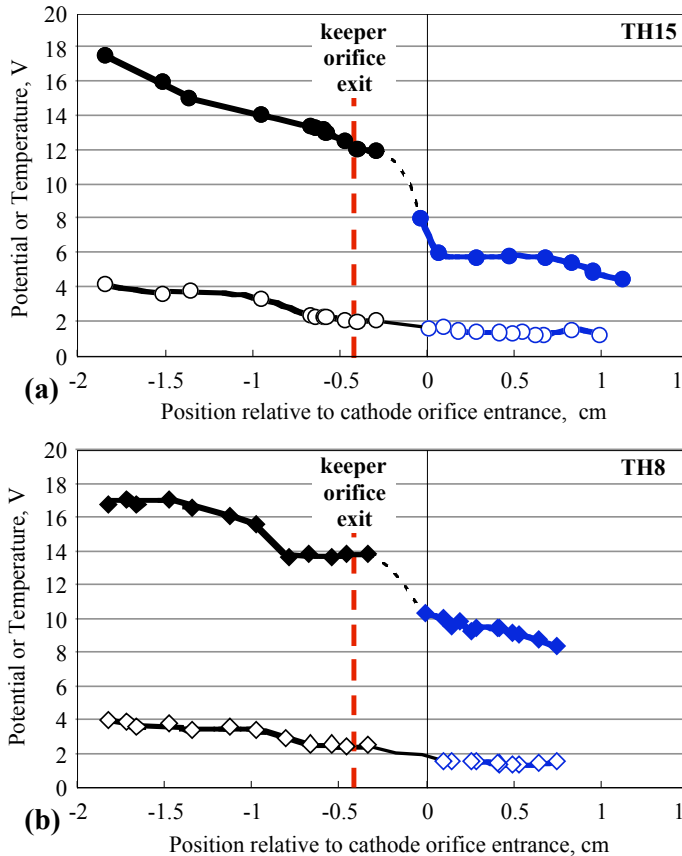


**Figure 12. Plasma potential and electron temperature for the cathode-keeper region for TH15 in (a) and TH8 in (b).**

and keeper region is also found not to be the highest in the system. The potential is also constant in the keeper orifice, and then increases downstream of the keeper orifice. This potential profile may be due to a relatively low current density in the large-orifice hollow cathode used in these experiments, which is less than  $600 \text{ A/cm}^2$  at discharge currents up to 35 A. The potential distribution observed in the cathode slowly increases to a maximum of about 30 V several cm downstream of the keeper. This is due to both the structure of the cathode plume and the increasing electron temperature observed as the probe moves downstream. The peak potential is about 3.2 V higher

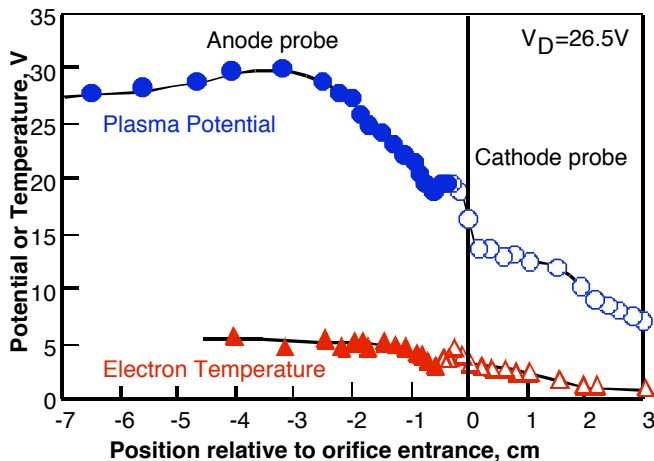


**Figure 13. Plasma potential and temperature profiles for the 25 A, 5.5 sccm case.**

the anode. The second potential discontinuity is established in the potential profile to generate more plasma by providing sufficient ionization to carry the current to the anode, and then the plasma potential continues to increase downstream of this region. Measurements downstream of 2 cm have been found by both Herman<sup>7,8</sup> and Sengupta<sup>9</sup> with these potential and electron temperatures for this region agree with both experiments.

The plasma potential and temperature profiles for the nominal NEXIS operation condition are shown in Fig. 13. In this experiment, the segmented conical anode was used and the discharge ran at 26.5 V, 25 A for 5.5 sccm of cathode flow. The plasma potential inside the hollow cathode on axis is found to be about 13 eV. The anode probe for this scan measured a plasma potential of about 19 V, which is slightly lower than the cathode probe due to radial mis-alignment of the probe estimated to be on the order of 0.5 mm. A 1 V difference is essentially the accuracy of the plasma potential measurement for this region, the difference is in the error bars for the probe. For the NEXIS cathode, there is also a potential discontinuity in the cathode orifice to the keeper orifice although the probe allows measurements in this region. The potential discontinuity is normally in the 5 to 10 V range and the plasma potential in the orifice

potential then falls downstream of the peak as the plasma density decreases further. Electron temperatures on the order of 2 to 3 eV are found inside the cathode insert and 4 to 6 eV are measured in the anode region.

The potential distribution in the anode region also changes with flow rate. Figure 14 shows the complete plasma potential and electron temperature profiles for the 25 A, 10 sccm case. Higher flow rates at a given current tend to push the observed potential discontinuity further downstream in the orifice. It is likely that smaller orifice diameters will also push the potential discontinuity down stream at the same flow rate due to the higher neutral density in the insert and orifice region. However, another

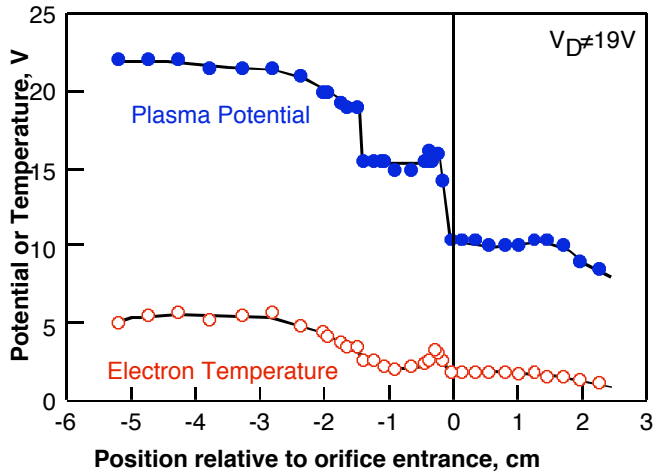


Figure 14. Plasma potential and electron temperature profiles from the 25A, 10 sccm case.

potential discontinuity is observed downstream about 1 cm from the keeper exit. This profile is looks similar to the NSTAR TH8 case, however the mechanism that produces the second potential discontinuity is different. Figure 15 shows the visible emission or plasma ball from the NSTAR cathode for TH4 TH8, TH12, and TH15; while Figure 16 shows the plasma ball for the NEXIS cathode at 25 A for 5.5 and 10 sccm. Exterior to the keeper, the axial extent of the plasma ball changes dramatically with flow and discharge current, and this effect can be seen in both Figs. 15 and 16. Higher flows tend to move the ball downstream, often exposing a classic Faraday dark space between the ball and the plasma located between the keeper and the cathode orifices. Higher currents tend to enlarge the

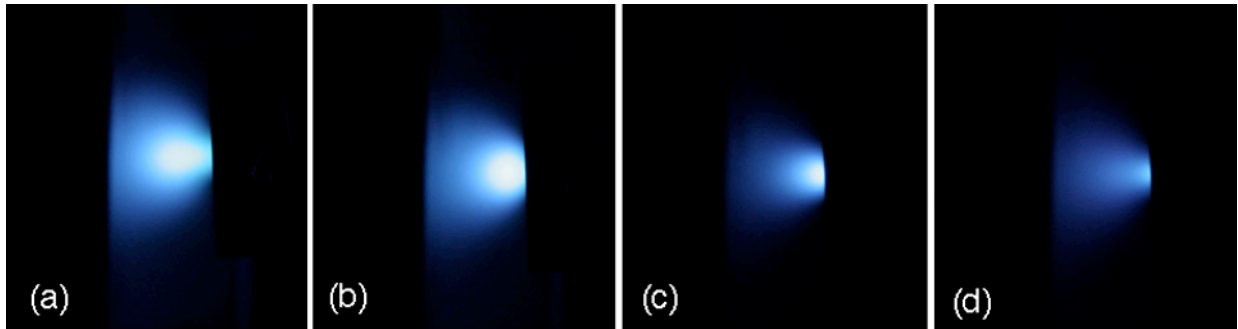


Figure 15. Plasma ball for TH15 (a), TH12 (b), TH8 (c), and TH4 (d).

ball, as does the application of an axial magnetic field, due to enhanced ionization. The plasma ball extends from the keeper orifice out a few millimeters downstream into the anode plasma. From Fig. 15, the pictures progress to lower throttle levels it can be seen that the plasma-ball is pulled into the keeper. During TH8 the ball is pulled partially inside the keeper and just tail end of the ball can be seen at the downstream end of the keeper orifice, which can be seen in Fig. 13(c). This suggests there is weak ionization just downstream of the keeper, leading to the potential profile seen in Fig. 12b. However the potential profile observed for the NEXIS cathode at 10 sccm, can be explained by Fig. 16b. The plasma ball is moved significantly downstream of the keeper orifice and at this high



Figure 16. Plasma ball for 25 A discharge for (a) 5.5 sccm and (b) 10 sccm.

flow rate a dark space is clearly observed. The dark space corresponds to a region of low electron temperature where excitation is decreased. However, this reduced-luminosity region also is observed in the 5.5 sccm case, although it is closer to the keeper and less apparent in the photograph. The constant potential for the 10 sccm case in the keeper orifice to 1 cm downstream can also be explained by the plasma not having sufficient energy to conduct to the anode due to the dark space observed in the photograph. Once

ionization is sufficient the potential jumps and the current can again be conducted to the anode.

#### IV. Discussion of the Plasma Profiles

Investigation of the cathode plasma and plume, show that plasma properties are significantly affected by cathode and anode geometries as well as operation conditions. The visible plasma ball present in both the NSTAR and NEXIS cathodes suggest that this area in the discharge chamber plays a significant role in conducting the current to the anode. The segmented conical anode allows the current to be measured for each individual section. For the NEXIS cathode at 5.5 sccm the current distribution shows that the majority of the current goes to the first ring and each consecutive ring decreases almost linearly. However, when the cathode flow is increased to 10 sccm, the first ring collects significantly less allowing each of the consecutive rings to collect more of the current. The same affect is seen when the diverging axial magnetic field is applied, the current collected by the first ring is decreased and the peak current is shifted downstream before the current begins to decrease almost linearly again.

The radial emissive and Langmuir probe allows the structure of the plasma ball to be investigated. From Fig. 15a, the NSTAR cathode at TH15, the plasma-ball is clearly visible and has a diameter slightly larger than 1 cm. From the emissive probe, the radial profile of the time-average plasma potential from emissive probe is shown in Fig. 17. The figure shows that the potential is depressed on axis in the cathode plume, and increases as the probe moves out radially. The potential starts to increase rapidly as the edge of the plasma ball is encountered, at about .5 cm. The plasma potential increases radially once the plasma gains enough energy to conduct the current to the anode, then the potential is relatively constant before it falls back to the anode potential.

The NEXIS cathode plume for 25 A at 5.5 sccm also shows a plasma ball similar to that of the NSTAR cathode at TH15. Using the Langmuir probe, radial potential profiles are shown in Fig. 18 for three different axial positions in the cathode plume. At 8.2 mm downstream of the cathode orifice the plasma ball seems to have the largest diameter with the potential increasing as the edge of the plasma ball is encountered. As the probe moves further downstream axially, the radial potential begins flatten out showing that the plasma ball is decreasing in physical size. In Fig. 16a, this can visibly be seen, the plasma is the most concentrated where the visible emission can be seen. This is also further illustrated in Fig. 19, where the density profiles for the NEXIS cathode for the same operation condition is shown.

The plasma density is concentrated on axis and as the probe moves out radially the density decreases in magnitude corresponding to the dispersion of plasma in to the anode region by the plasma ball and the density falls. Figure 19 also shows axially that the density falls an order of magnitude corresponding to Figure 10b.

In these experiments, the shape of the anode electrode strongly affected the discharge voltage. The original cylindrical anode produced typically 16 to 17 V discharges at the nominal 25 A and 5.5 sccm. Installing the conical anode geometry raised the anode voltage to 26 V, and produced the potential profiles previously shown in Fig. 13.

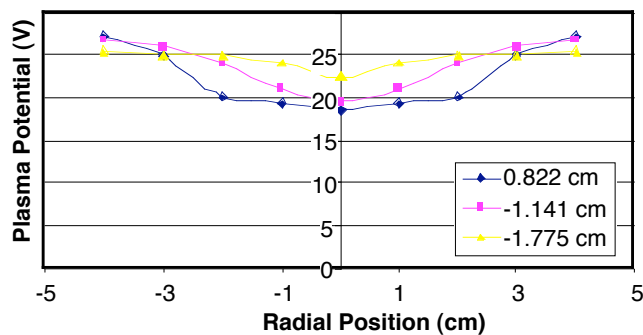


Figure 18. Plasma Potential radially for the NEXIS cathode for 25 A at 5.5 sccm.

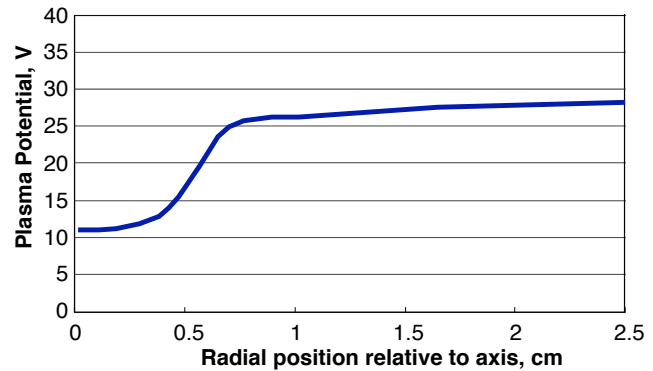
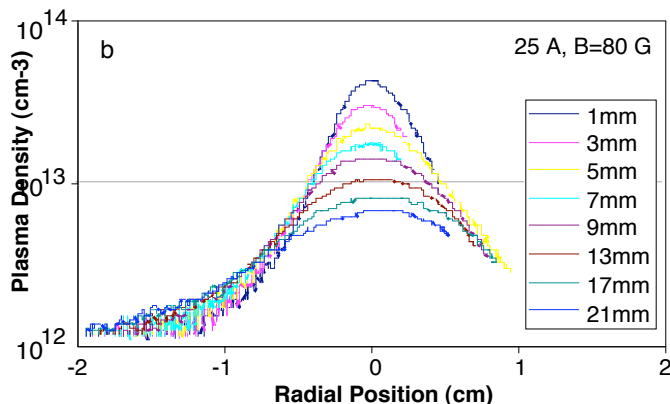


Figure 17. Time averaged radial profile of plasma potential for TH15 with an emissive probe.

The potential and temperature profiles in the cylindrical anode case at 25 A and 5.5 sccm are shown in Fig. 20. The plasma potential in the cathode insert and orifice regions is essentially unchanged. Modification of the anode geometry did not affect the basic cathode operation because these potentials and temperatures are sufficient to deliver the desired discharge current at the given cathode flow rate. The anode geometry changes modify only the potential exterior to the cathode in the anode-plasma region, where the potential quickly raises to about 4 V positive relative to the anode potential and is relatively flat over the scan range. The conical



**Figure 19. Plasma density radial profile for the NEXIS cathode for 25 A at 5.5 sccm.**

time, the discharge voltage at a given flow would increase 2 to 3 V, and then require on the order of 10 hours to fully recover. The probe data showed that the plasma potential inside the insert region tracked the discharge voltage. This is consistent with the work function depending on conditioning and on the history of the cathode surface. Environmental effects that might raise the work function are handled in the “self-heating” system by the plasma increasing the power delivered to the cathode, which increases the temperature to sufficient levels to produce the required electron emission. This conditioning and history dependence is planned to be studied to determine its impact on the life and reliability of hollow cathodes in ion thrusters.

## V. Conclusion

Probe studies of hollow cathode discharges have provided considerable insight into the plasma structure upstream and downstream of the cathode orifice, specifically the potential, density, temperature profiles through the system. The miniature scanning probes allowed high density regions to be investigated and mapped where the plasma was too intense for slow or stationary probes to be used. This work has demonstrated that the potential structure in hollow cathode discharges varies significantly with discharge current, flow rate, anode geometry and cathode geometry. Since the data presented here is only for two operation conditions for both the NSTAR and NEXIS hollow cathode geometry, future work will also expand on the operating conditions and geometry space to help construct a comprehensive model of the hollow cathode discharge. Also new proposed Discovery missions are interested in center feed Hall thrusters for their main propulsion systems, further modeling and experimental data on the hollow cathode discharges will aid in the design for life of Hall thrusters.

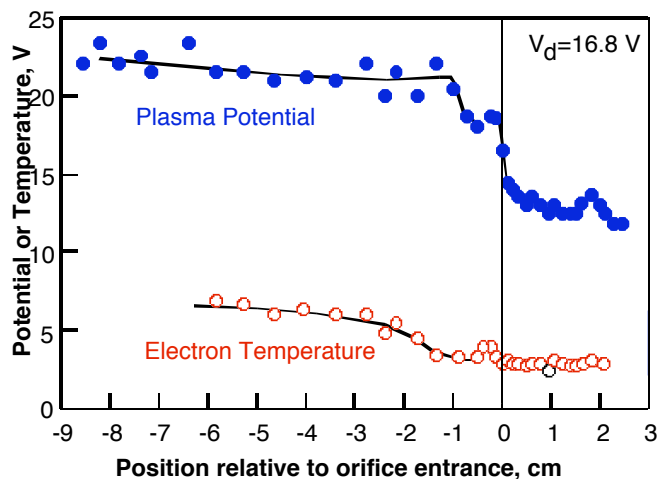


**Figure 20. Plasma potential and electron temperature for the nominal 25A case with the cylindrical anode.**

## Acknowledgments

The research described in this paper was carried out by the Jet Propulsion Laboratory, California Institute of Technology, under a contract with the National Aeronautics and Space Administration in support of Project Prometheus.

anode also showed 3 to 4 V plasma potentials above the anode voltage, but the discharge required higher voltages to generate the anode plasma and conduct the current the anode. This is likely because the gas density is significantly lower in the anode region in the conical anode case. This implies that larger thrusters with anodes farther away from the cathode will probably require higher cathode flow rates to operate at the same discharge voltages as small thrusters.

Finally, both hollow cathodes showed clear indications of long-term and short-term conditioning. When first turned on, the discharge voltage was observed to decrease slowly over several hundred hours and then stabilize. If exposed to air for any significant

## References

- <sup>1</sup>Lidsky, L., Rothleder, J. Rose, D., Yoshikawa, S., Michelson, C., Mackin, J. Appl. Phys. **22** (1962) p.2490.
- <sup>2</sup>Rawlin, V., Pawlik, E., "A Mercury Plasma Bridge Neutralizer", *J. Spacecraft Rockets*, **5** (1968) p.814.
- <sup>3</sup>Moore, R. "Magneto-Electrostatically Contained Plasma Ion Thruster", AIAA Paper #69-260, 7<sup>th</sup> Electric Propulsion Conference, Williamsburg, VA, March 3-5, 1969.
- <sup>4</sup>Sovey, J. "Performance of a Magnetic Multipole Line-Cusp Argon Ion Thruster", AIAA Paper #81-0745, AIAA Electric Propulsion Conference, Las Vegas, Nevada, April 21-23, 1981.
- <sup>5</sup>Siegfried, D. and Wilbur, P., "An Investigation of Mercury Hollow Cathode Phenomena", AIAA Paper #78-705, 13<sup>th</sup> International Electric Propulsion Conference, San Diego, CA, April 25-27, 1978.
- <sup>6</sup>Hayakawa, Y., Miyazaki, K., Kitmuira, S., "Measurements of Electron Energy Distributions in a 14 cm Diameter Ring-Cusp Ion Thruster", AIAA Paper #89-2715, 25<sup>th</sup> Joint Propulsion Conference, Monterey, CA July 10-12, 1989.
- <sup>7</sup>D.Herman and A.Gallimore, "Discharge Chamber Plasma Structure of a 30-cm NSTAR Ion Engine", AIAA Paper #2004-3794, 40<sup>th</sup> Joint Propulsion Conference, Ft. Lauderdale, FL, July 11-14, 2004.
- <sup>8</sup>D.Herman and A.Gallimore, "Comparison of Discharge Plasma Parameters in a 30-cmNSTAR Type Ion Engine with and without Beam Extraction", AIAA Paper #2003-5162, 39<sup>th</sup> Joint Propulsion Conference, Huntsville, AL, July 20-23, 2003.
- <sup>9</sup>A.Sengupta, D.M. Goebel, D. Fitzgerald, A. Owens, "Experimentally Determined Neutral Density and Plasma Parameters in a 30 cm Ion Engine", AIAA Paper #2004-3613, 40<sup>th</sup> Joint Propulsion Conference, Ft. Lauderdale, FL, July 11-14, 2004.
- <sup>10</sup>D.Herman and A.Gallimore, "Near Discharge Cathode Assembly Plasma Potential Measurements in a 30-cm NSTAR-type Ion Engine amidst Beam Extraction", AIAA Paper #2004-3958, 40<sup>th</sup> Joint Propulsion Conference, Ft. Lauderdale, FL, July 11-14, 2004.
- <sup>11</sup>D.M.Goebel, K.Jameson, R.Watkins, I.Katz, "Hollow Cathode and Keeper-Region Plasma Measurements Using Ultra-Fast Miniature Scanning Probes", AIAA Paper #2004-3430, 40<sup>th</sup> Joint Propulsion Conference, Ft. Lauderdale, FL, July 11-14, 2004.
- <sup>12</sup>K.K. Jameson, D.M. Goebel, R. Watkins, "Hollow Cathode and Keeper-Region Plasma Measurements", AIAA Paper #2005-3667, 41<sup>th</sup> Joint Propulsion Conference, Tuscan, AZ, July 10-13, 2005.
- <sup>13</sup>A. Sengupta, J. Brophy, K. Goodfellow, "Status of the Extended Lift Test of the Deep Space 1 Flight Spare Ion Engine After 30'352 Hours of Operation", AIAA Paper #2003-4558, 39<sup>th</sup> Joint Propulsion Conference, Huntsville, AL, July 20-23, 2003.
- <sup>14</sup>J. Brophy, "NASA's Deep Space 1 Ion Engine", *Rev. Sci.Instrum.* **73** (2002) p.1071-1078
- <sup>15</sup>F.Chen, "Electric Probes", in *Plasma Diagnostics Techniques* (ed. R. Huddelstone and S. Leonard), Academic Press, NY (1966) p. 113-200.
- <sup>16</sup>D.Bohm, *The Characteristics of Electrical Discharges in Magnetic Fields*, edited by A. Gutirie and R.K. Wakerling (McGraw-Hill, New York, 1949) Chap.3.
- <sup>17</sup>I. Katz, et al., "Combined Plasma and Thermal Hollow Cathode Insert Model" IEPC 2005-228, International Electric Propulsion Conference, Princeton, NJ, Oct.31<sup>st</sup>-Nov.4<sup>th</sup>, 2005.